Electronic Supplementary Information (ESI)

Charge Effect of Foreign Metal Ions and Crystal Growth Process in Hybridized Metal-Organic Frameworks

Woo Ram Lee, Dae Won Ryu, Won Ju Phang, Ji Hye Park, and Chang Seop Hong*

Department of Chemistry, Research Institute for Natural Sciences, Korea University, Seoul 136-713, Korea; E-mail: cshong@korea.ac.kr

Experimental Details

Preparations. The organic material H_3TPO was prepared by using the literature method.[s1]

[Cu(HTPO)](DMF)$_2$(H$_2$O)$_{1.5}$ (CuHTPO; 1): H_3TPO (100 mg, 0.24 mmol), Cu(NO$_3$)$_2$·6H$_2$O (88 mg, 0.37 mmol), 5 mL of mixed solvent (DMF:H$_2$O:MeOH=3:3:1), and a few amount of HNO$_3$ were located together in a 10 mL vial. The vial was sealed tightly and placed in a preheated oven at 70 °C. After 48 h, green crystals precipitated. The crystals were separated by filtration and washed with mixed solvent (DMF:H$_2$O:MeOH = 3:3:1). Yield: 85%. Elemental analysis (%) calcd for C$_{27}$H$_{30}$CuN$_2$O$_{10.5}$P: C 50.27, H 4.69, N, 4.34; found: C 50.53, H 4.23, N 4.12.

ZnTPO/CuHTPO: CuHTPO (20 mg, 0.031 mmol), Zn(NO$_3$)$_2$·6H$_2$O (149 mg, 0.5 mmol), and 1 mL of mixed solvent (DMF:H$_2$O:MeOH = 3:3:1) were put together in a 10 mL vial. The sealed vial was located in an oven at 100 °C. After 72 h, core-shell type crystals were formed. The crystals were filtered and washed with mixed solvent (DMF:H$_2$O:MeOH = 3:3:1). The shell crystal was carefully cut to collect single-crystal X-ray diffraction data and analyzed as (H$_3$O)$_2$[Zn$_{15}$(TPO)$_8$(OH)$_6$(O)] (**ZnTPO; 2**). The structure with a chemical formula of H[(Zn$_3$(OH)(H$_2$O)$_3$)(TPO)$_2$], reported in the literature,[s2] was afforded by using the same experimental conditions in the absence of **CuHTPO**.

TbTPO/CuHTPO: CuHTPO (20 mg, 0.031 mmol) and Tb(NO$_3$)$_3$·5H$_2$O (218 mg, 0.5 mmol) were put in a 10 mL vial (1 mL mixed solvent of DMF:H$_2$O:MeOH=3:3:1). The vial was sealed tightly and located in a preheated oven at 100 °C. After 72 h, core-shell crystals were formed. The crystals were collected by filtration and washed with mixed solvent (DMF:H$_2$O:MeOH = 3:3:1). The shell part, (H$_3$O)[Tb$_2$(TPO)$_2$(formate)] **(TbTPO; 3),** was carefully cut to study single-crystal X-ray diffractions. The Tb complex was alternatively prepared as a following method: H_3TPO (100 mg, 0.24 mmol), Tb(NO$_3$)$_3$·5H$_2$O (104 mg, 0.24 mmol) were placed in 5 mL of mixed solvent

(DMF:H_2O:MeOH=3:3:1), and a few amount of HNO_3 were located together in a 10 mL vial. The sealed vial was put in a preheated oven at 100 ^{o}C. After 24 h, block shaped colorless crystals were produced. The crystals were isolated by filtration and washed with mixed solvent (DMF:H_2O:MeOH = 3:3:1). Yield: 70%. Elemental analysis (%) calcd for $C_{55.6}H_{59.8}TbN_{4.2}O_{22.4}P_2Tb_2$: C 43.79, H 3.95, N 3.86; found: C 43.30, H 4.58, N 4.23.

Crystallographic Structure Determination. X-ray data for **1 - 3** were collected on a Bruker SMART APEXII diffractometer equipped with graphite monochromated MoKα radiation (λ = 0.71073 Å). Preliminary orientation matrix and cell parameters were determined from three sets of ω scans at different starting angles. Data frames were obtained at scan intervals of 0.5^o with an exposure time of 10 s per frame. The reflection data were corrected for Lorentz and polarization factors. Absorption corrections were carried out using SADABS.[s3] The structures of **1 – 3** were solved by direct methods and refined by full-matrix least-squares analysis using anisotropic thermal parameters for non-hydrogen atoms with the SHELXTL program.[s4] Guest molecules in **1 - 3** are significantly disordered and could not be modeled properly, thus the program SQUEEZE,[s5] a part of the PLATON package of crystallographic software,[s6] was used to calculate the solvent disorder area and remove its contribution to the overall intensity data. For **1**, the contributions of some 548 electrons were removed from the unit-cell contents, and as Z = 8 in this case, this could/might correspond with the removal of solvent such as 1(DMF) and 3(H_2O) [some 69 electrons] from the Cu(II) formula unit. For **2**, the contributions of some 1259 electrons were removed from the unit-cell contents. The oxygen (O4) atom is at a site with -3 symmetry and there are six Zn(II)$_{2.5}$ formula units in the unit cell. Therefore, this could/might correspond with the removal of solvent such as 5(DMF) and 1(H_2O) [some 210 electrons] from the Zn(II)$_{2.5}$ formula unit. The water and carboxylate oxygens were disordered over two sites (0.61:0.39 for O8A and O8B; 0.5:0.5 for O3A and O3B), respectively. For **3**, the contributions of some 199 electrons were removed from the unit-cell contents, and as Z = 2 in this case, this could/might correspond with the removal of solvent such as 2(DMF) and 2(H_2O) [some 100 electrons] from the Tb(III)$_2$ formula unit. All hydrogen atoms except for hydrogens bound to water oxygens were calculated at idealized positions and refined with the riding models. Crystal data of **1**(squeezed): empirical formula = $C_{23.88}H_{26}CuNO_{11}P$, Mr = 597.47, T = 130 K, orthorhombic, space group *Pbcn*, a = 16.0811(4) Å, b = 24.0918(6) Å, c = 14.2992(4) Å, V = 5539.8(2) Å^3, Z = 8, D_{calc} = 1.433 g cm^{-3}, μ = 0.904 mm^{-1}, 83887 reflections collected, 6858 unique (R_{int} = 0.0536), $R1$ = 0.0438, $wR2$ = 0.1332 [$I > 2\sigma(I)$]. **2**(squeezed): empirical formula = $C_{258}H_{384}N_{13.33}O_{129}P_8Zn_{15}$, Mr = 6964.76, T = 100 K, trigonal, space group *R-3*, a = 34.340(3) Å, c = 19.451(2) Å, V = 19865(4) Å^3, Z = 3, D_{calc} = 1.747 g cm^{-3}, μ = 1.493 mm^{-1}, 27880 reflections collected, 10904 unique (R_{int} = 0.0935), $R1$ = 0.0792, $wR2$ = 0.2103 [$I > 2\sigma(I)$]. **3**(squeezed): empirical formula = $C_{49}H_{44.5}N_2O_{21}P_2Tb_2$, Mr = 1377.15, T = 296 K, monoclinic, space group *P2/n*, a = 14.4794(6) Å, b = 10.5573(5) Å, c = 23.3160(11) Å, β = 107.316(3)^o, V = 3402.6(3) Å^3, Z = 2, D_{calc} = 1.344 g cm^{-3}, μ = 2.171 mm^{-1}, 28623 reflections collected, 8407 unique (R_{int} = 0.0664), $R1$ = 0.0447, $wR2$ = 0.1007 [$I > 2\sigma(I)$].

Physical Measurements. Elemental analyses for C, H, and N were performed at the Elemental Analysis Service Center of Sogang University. Infrared spectra were obtained from KBr pellets with a Bomen MB-104 spectrometer.

Thermogravimetric analyses were carried out at a ramp rate of 10 ^{o}C/min in a N_2 flow using a Scinco TGA N-1000 instrument. PXRD data were recorded using Cu Kα ($\lambda = 1.5406$ Å) on a Rigaku Ultima III diffractometer with a scan speed of 2°/min and a step size of 0.01^{o}. Photoluminescence were measured with a Hitachi F-7000 FL spectrophotometer. The ICP data were collected on ICP-AES (ICP-OES; JY Ultima2C; Jobin Yvon, France) spectrometer.

Gas Sorption Measurements. Gas sorption isotherms were measured using a BEL Belsorp mini II gas adsorption instrument up to 1 atm of gas pressure. The desolvated sample **1** was obtained by heating **CuHTPO** at 160 ^{o}C under vacuum for 16 h. The highly pure N_2 (99.999%), H_2 (99.999%), CO_2 (99.999%), CH_4 (99.995 %), CO (99.998%), and O_2 (99.995%) were used in the sorption experiments. N_2 and H_2 gas isotherms were measured at 77 K and CO_2 was measured at 195 K. For H_2, the additional uptake isotherm was obtained at 87 K to calculate heats of adsorption.

References

s1. W.-N. Chou and M. J. Pomerantz., *Org. Chem.* 1991, **56**, 2762.

s2. S. M. Humphrey, S. E. Oungoulian, J. W. Yoon, Y. K. Hwang, E. R. Wise and J.-S. Chang, *Chem. Commun.* 2008, 2891.

s3. G. M. Sheldrick, 1994, SADABS, A program for area detector absorption corrections, University of Göttingen, Germany.

s4. G. M. Sheldrick, 1995, SHELXTL, version 5, Bruker AXS, Madison, Wisconsin.

s5. P. van der Sluis and A. L. Spek, *Acta Crystallogr.* 1990, **A46**, 194.

s6. A. L. Spek, *Acta Cryst.* 1990, **A46**, 1.
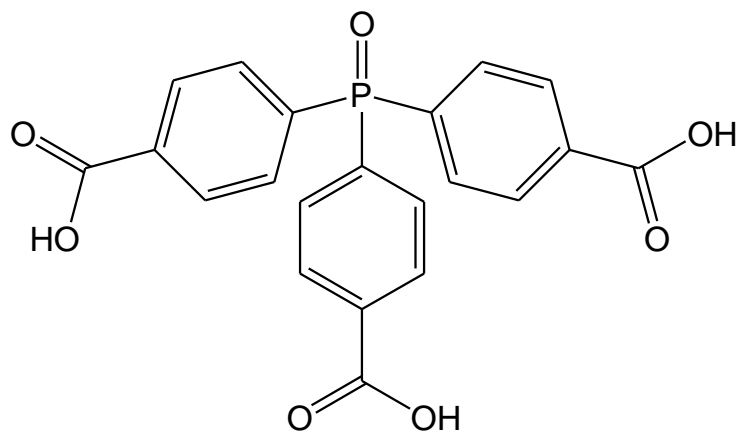
H$_3$TPO
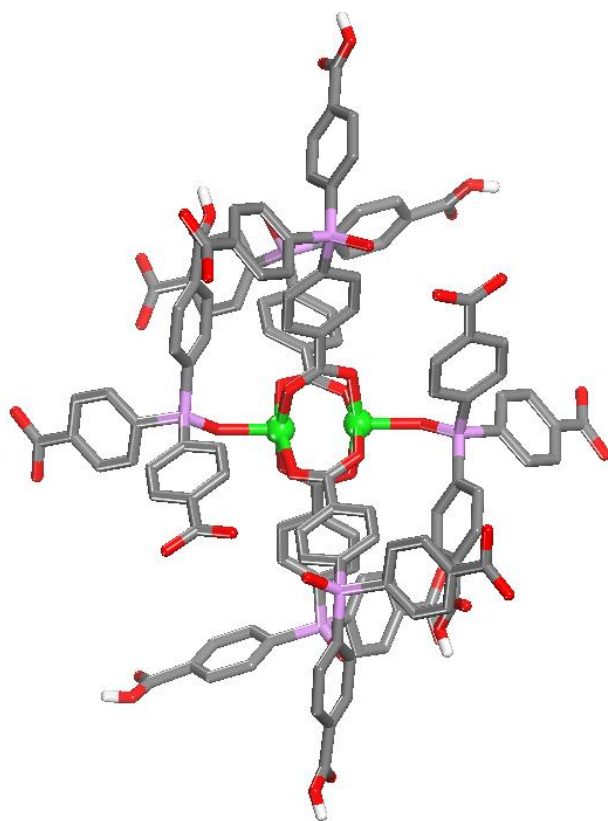
Fig. S1. (top) Structure of H$_3$TPO and (bottom) molecular view showing the geometric environment around the Cu$_2$(CO)$_4$ SBU of **CuHTPO**.
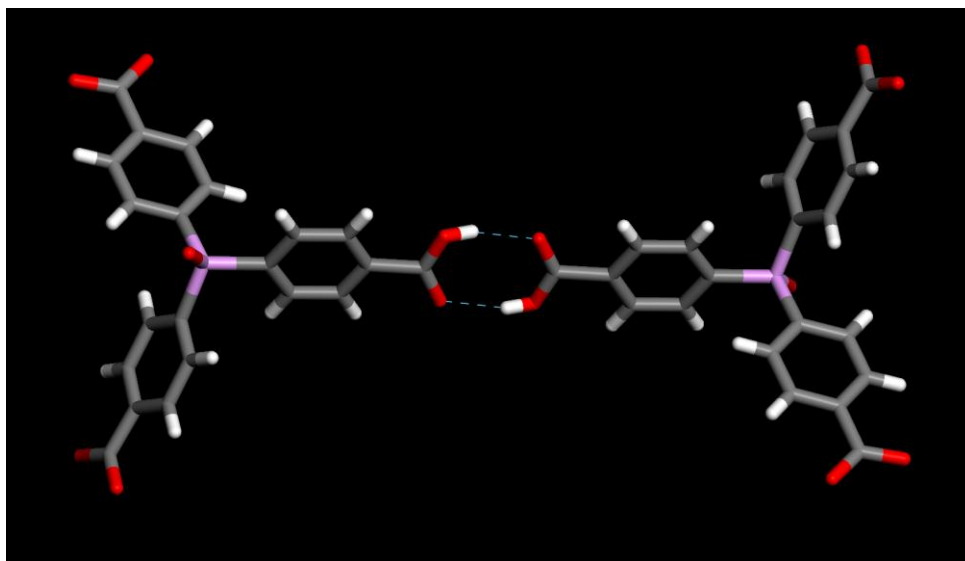
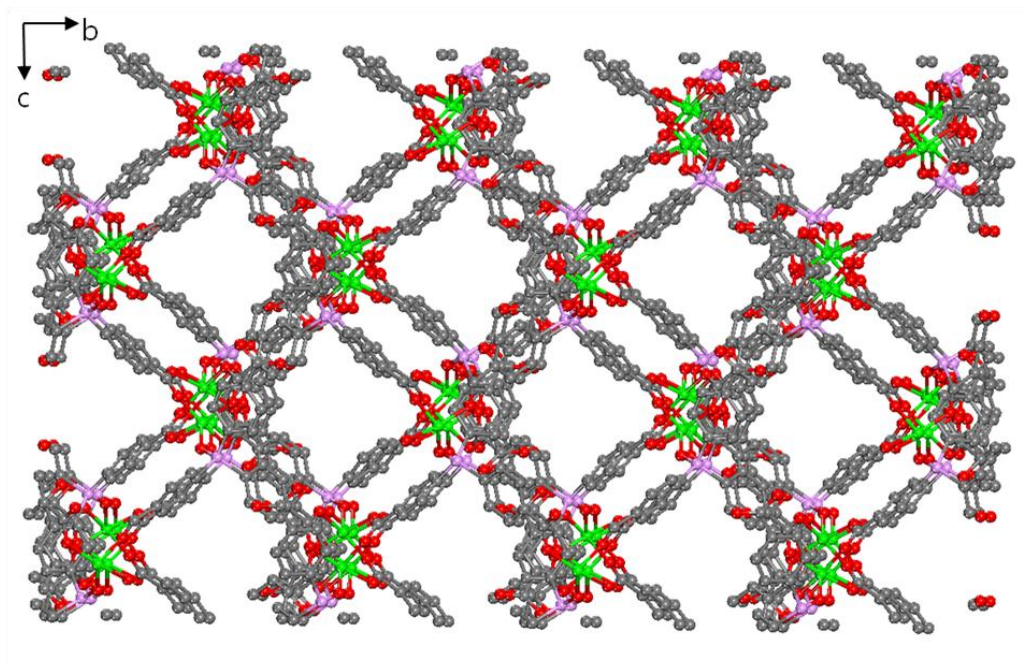Fig. S2. Structure of dimeric (HTPO)$_2$ unit through hydrogen bonding in **CuHTPO**.

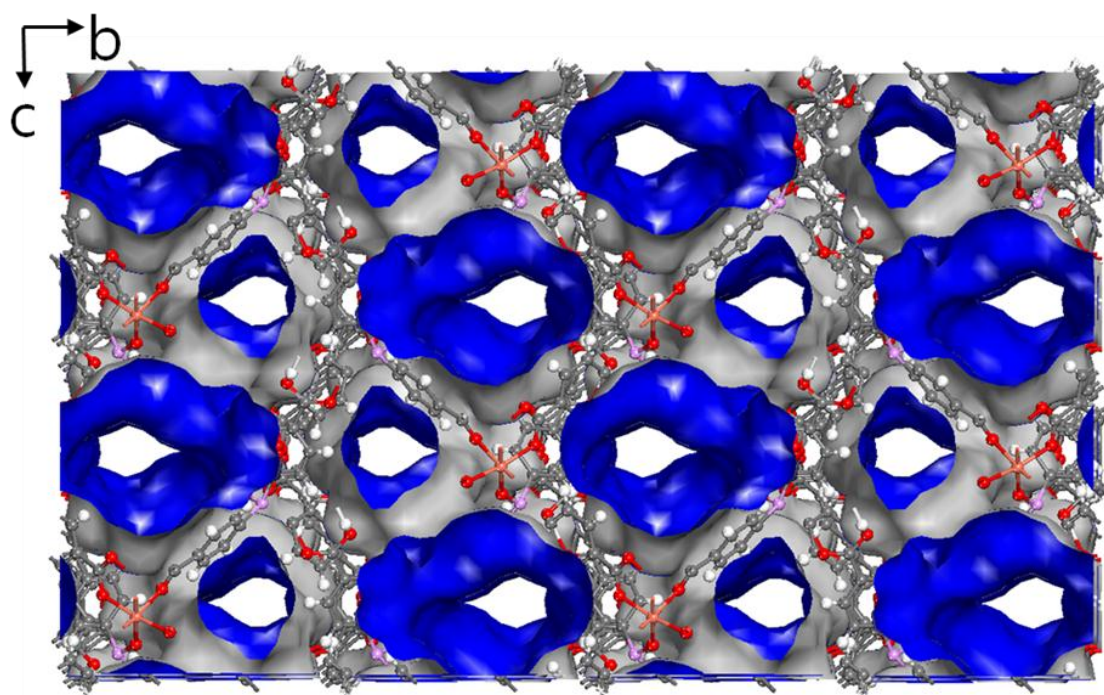Fig. S3. Three-dimensional network of **CuHTPO** in the *bc* plane.

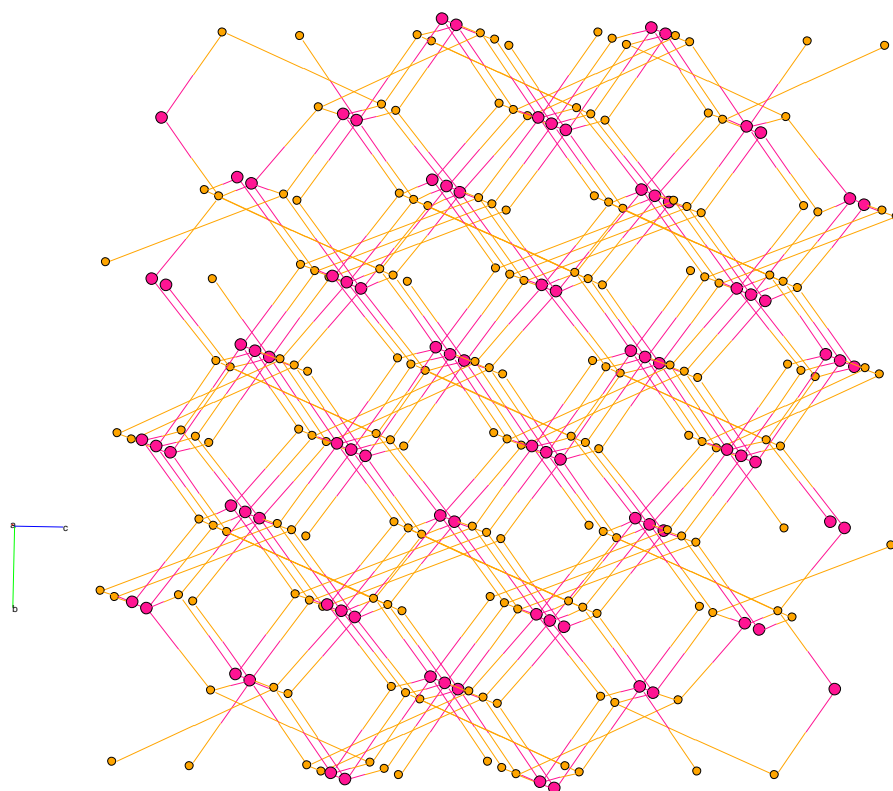Fig. S4. Connolly surface diagram with 1D channels running down the a-axis.
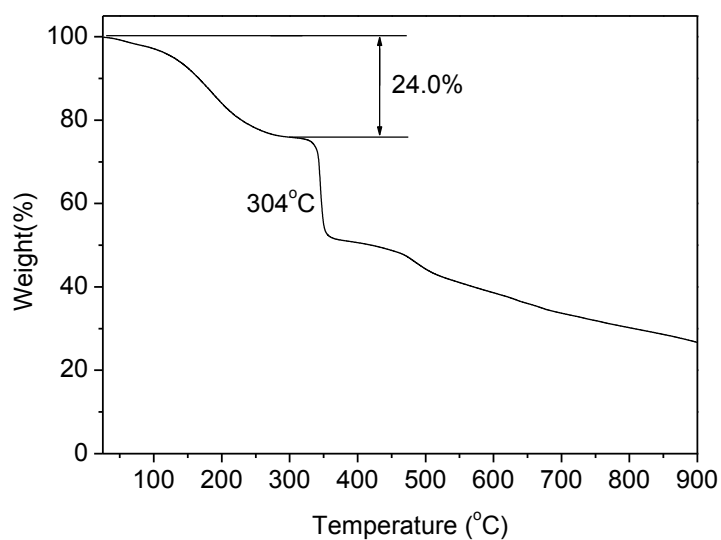
Fig. S5. Simplified net of **CuHTPO**.

Fig. S6. TGA data for **CuHTPO**. A weight loss of 24% in thermogravimetric analysis (TGA) on **CuHTPO** corresponds to removal of 0.5 H_2O and 2 DMF molecules in the temperature range of 27 – 300 ^{o}C. The framework remains intact up to 310 ^{o}C.
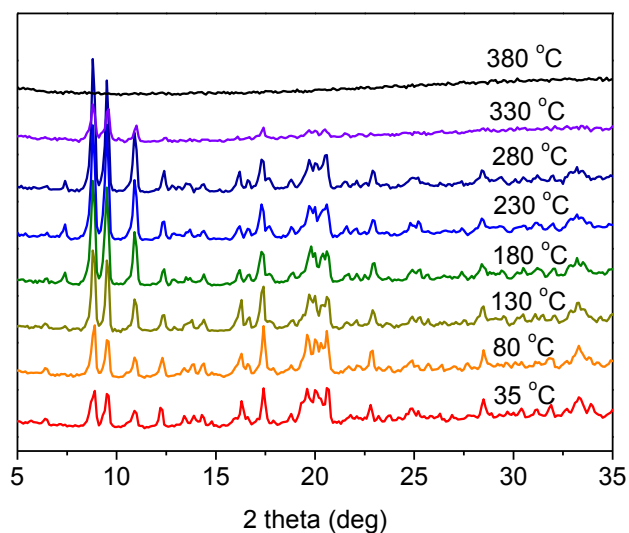
Fig. S7. PXRD profiles with indicated temperatures for **CuHTPO**. The framework integrity up to 310 ^{o}C was confirmed by the variable temperature PXRD data.

8
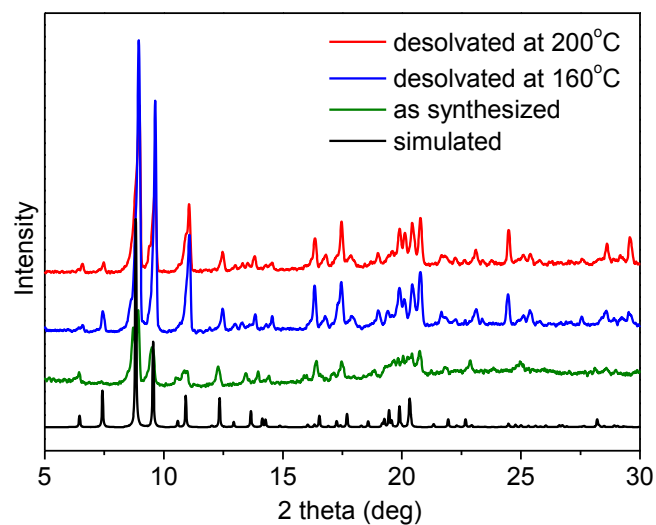
Fig. S8. PXRD profiles for simulated, **CuHTPO**, desolvated **CuHTPO** at 160 and 200 ^{o}C under vacuum for 16 h. The structural integrity is retained at both conditions.
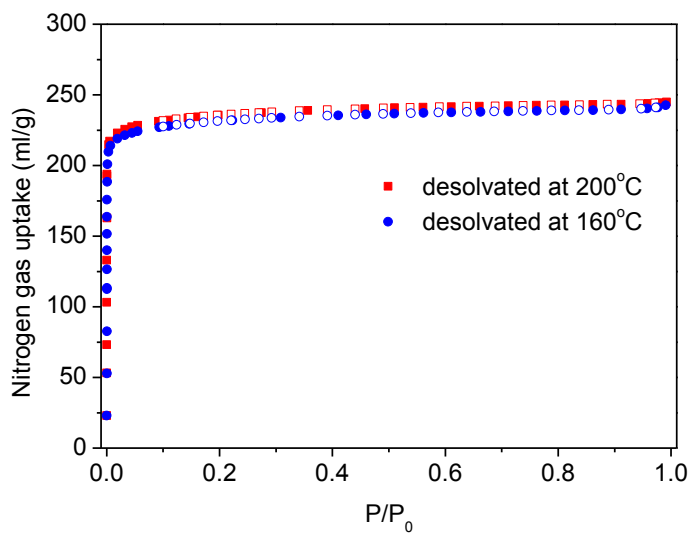
Fig. S9. N_2 sorption isotherms of desolvated **CuHTPO** activated at different temperatures. The adsorption capacity is almost same at the two temperatures. The structural integrity is retained at both conditions with identical sorption capacity.
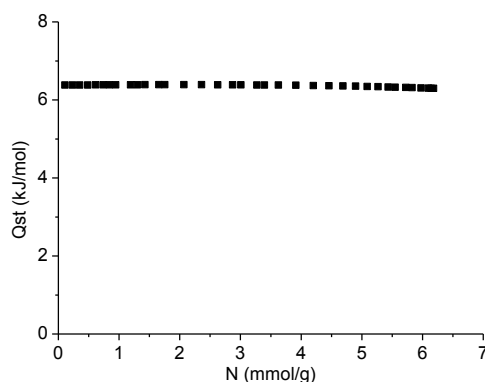
9
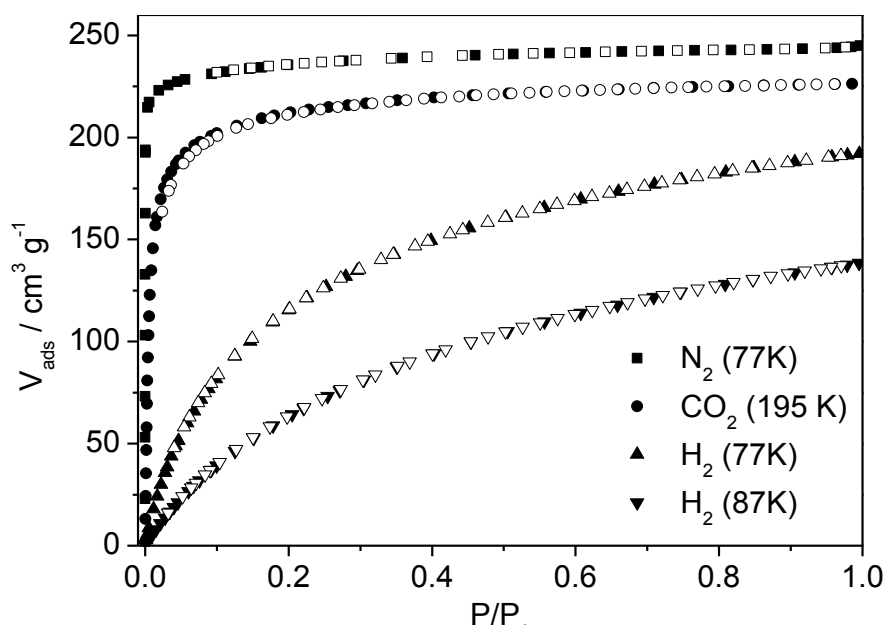
Fig. S10. Adsorption isotherms of desolvated **CuHTPO** with several gas molecules. Permanent microporosity is verified by measuring the N_2 sorption isotherm for **CuHTPO**, which shows a characteristic type I curve. From this plot, the Brunauer-Emmett-Teller (BET) surface area and total pore volume are extracted to be 950 m^2/g and 0.38 cm^3/g, respectively. For H_2 and CO_2 uptake, the maximum amounts at 1 atm and 77 K are equal to 8.57 mmol/g (192 cm^3/g) and 10.1 mmol/g (226 cm^3/g), which are equivalent to the number of gas molecules per formula unit being 4.0 and 4.8, respectively.

(a)

	Value	Standard E
a0	-767.3028	1.51154
a1	-0.9208	0.48374
a2	0.08283	0.16404
a3	0.04293	0.02908
a4	0.00172	0.00167
a5	0	0
a6	0	0
a7	0	0
b0	12.2361	0.01823
b1	0.20507	0.00474
b2	0	0
b3	0	0
b4	0	0
b5	0	0
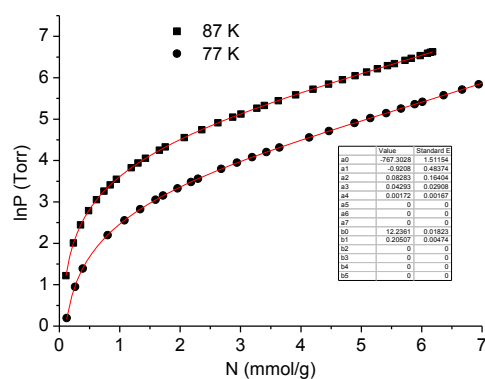
(b)

Fig. S11. (a) H_2 isotherms at 77 K and 87 K, and virial equation fits for desolvated **CuHTPO**. (b) Plot of the isosteric heat of H_2 adsorption for desolvated **CuHTPO**.

The H_2 adsorption data at two temperatures were fitted using the virial-type equation with a_i and b_i parameters,

$$ln\ P = ln\ N + (1/T)\Sigma_{i=0}^{r}(a^i N^i) + \Sigma_{i=0}^{s}(b^i N^i) \tag{1}$$

where P is the pressure in Torr, N is the amount adsorbed in mmol/g, T is the temperature in K, a_i and b_i are virial coefficients, and r and s are the number of coefficients required to express the isotherms. The fitted coefficients a_0 through a_r were then applied to estimate the isosteric heat of adsorption using the following expression

$$Q_{st} = -R\Sigma_{i=0}^{r}(a^i N^i) \tag{2}$$

where Qst is the isosteric heat of adsorption depending on the coverage and R is the universal gas constant.

The data were fitted with a virial-type equation to give the adsorption enthalpy of 6.3 – 6.4 kJ/mol. This value is analogous to those of metal-carboxylate or metal-cyanide MOFs.[s7]

s7. a) D. M. D'Alessandro, B. Smit and J. R. Long, *Angew. Chem. Int. Ed.* 2010, **49**, 6058-6082. b) J.-R. Li, R. J. Kuppler and H.-C. Zhou, *Chem. Soc. Rev.* 2009, **38**, 1477-1504. c) L. Ma, C. Abney and W. Lin, *Chem. Soc. Rev.* 2009, **38**, 1248-1256. d) L. J. Murray, M. Dincă and J. R. Long, *Chem. Soc. Rev.* 2009, **38**, 1294-1314.
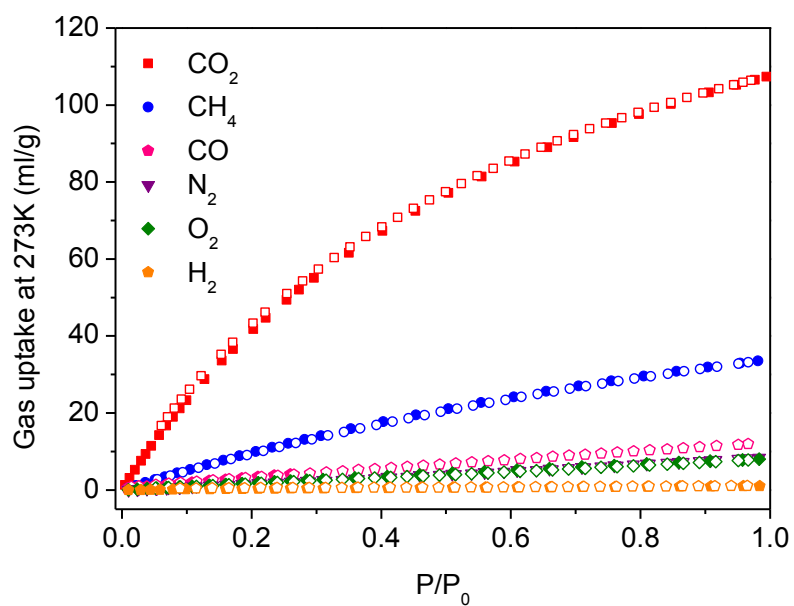
Fig. S12. Several gas isotherms of the deslovated **CuHTPO** at 273 K. The uptake ratios of CO_2 over the other gases at 1 atm are 3.2 for CO_2/CH_4, 8.9 for CO_2/CO, 13.4 for CO_2/N_2 and CO_2/O_2, and 107.1 for CO_2/H_2. The higher capacity of CO_2 is related to the greater quadrupole moment and polarizability of CO_2 compared to the other gas molecules.
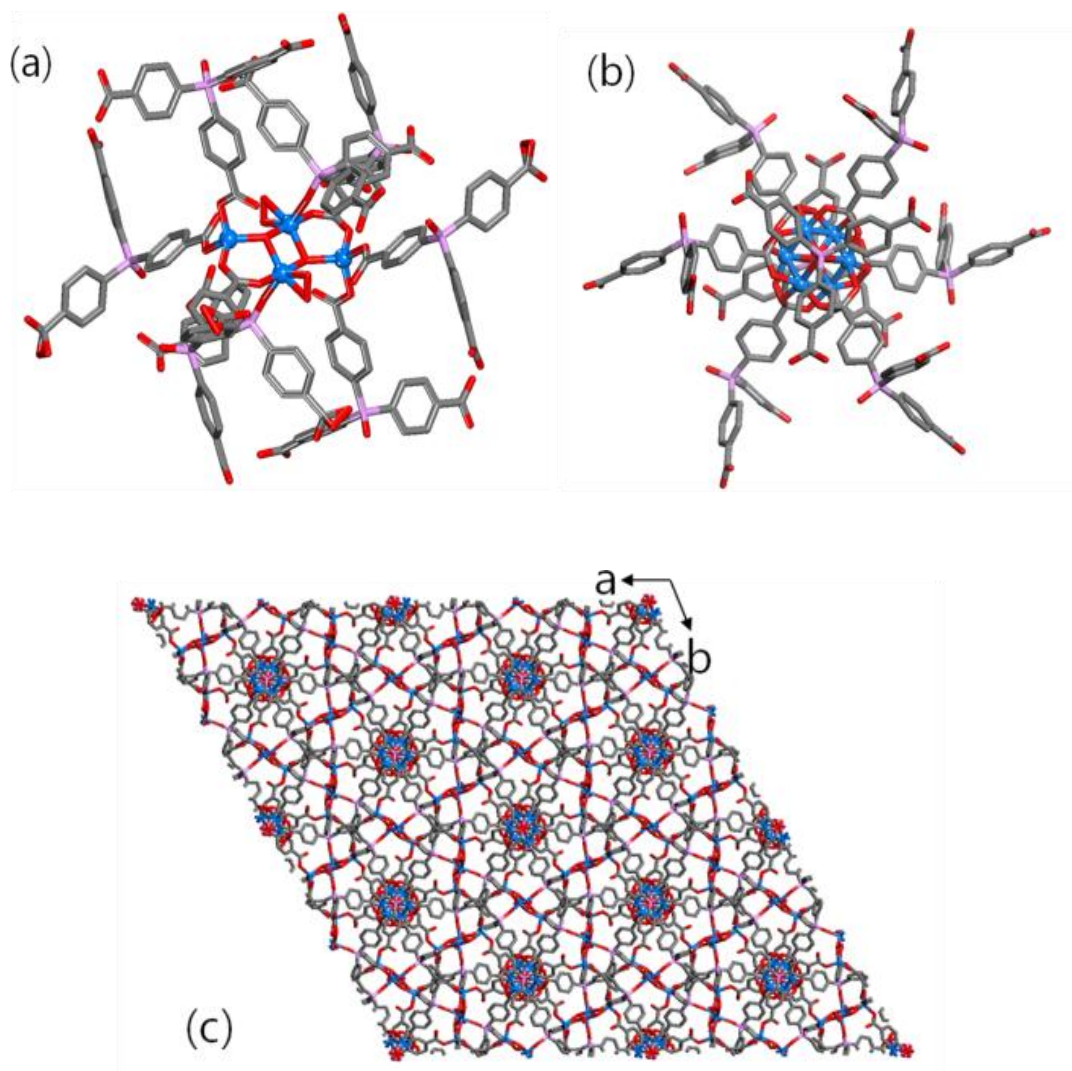
Fig. S13. Building nodes of a) $Zn_4(OH)_2(H_2O)_2(TPO)_8$ and b) $Zn_3(O)(TPO)_8$ for **ZnTPO**. Zn and carboxylate oxygens are disordered. c) Extended 3D view in the *ab* plane.
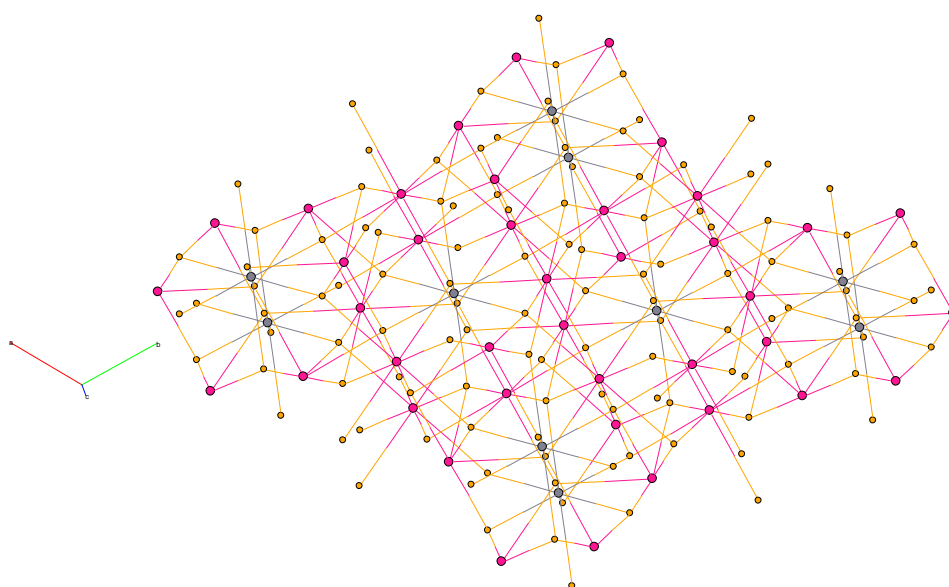
Fig. S14. Simplified net of **ZnTPO**.
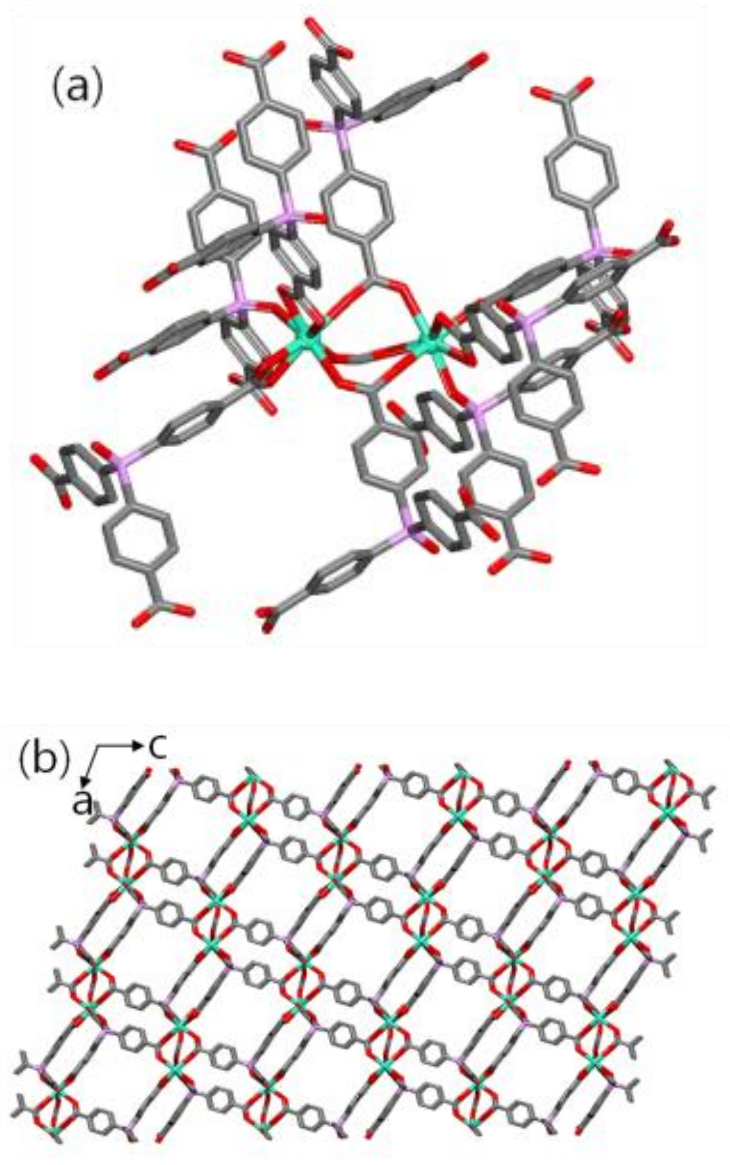
Fig. S15. a) Building unit of Tb_2(formate)$(TPO)_8$ for **TbTPO**. b) Extend structural view in the *ac* plane.
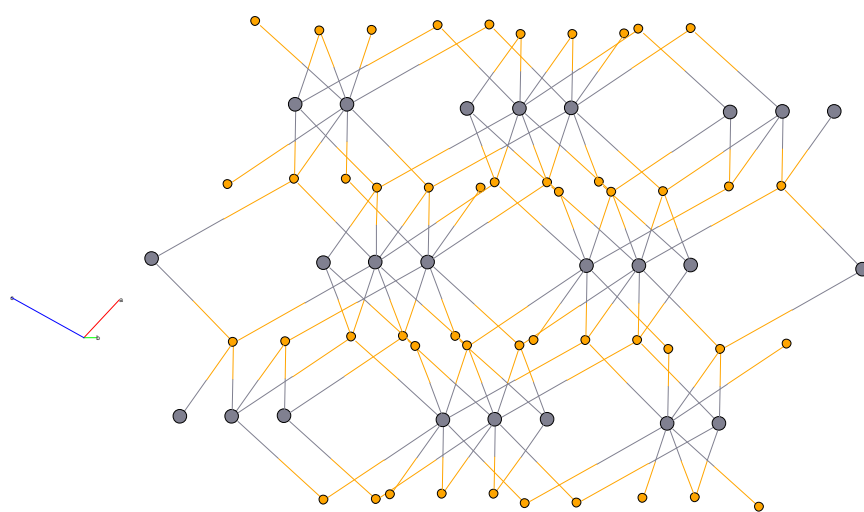
Fig. S16. Simplified net of **TbTPO**.
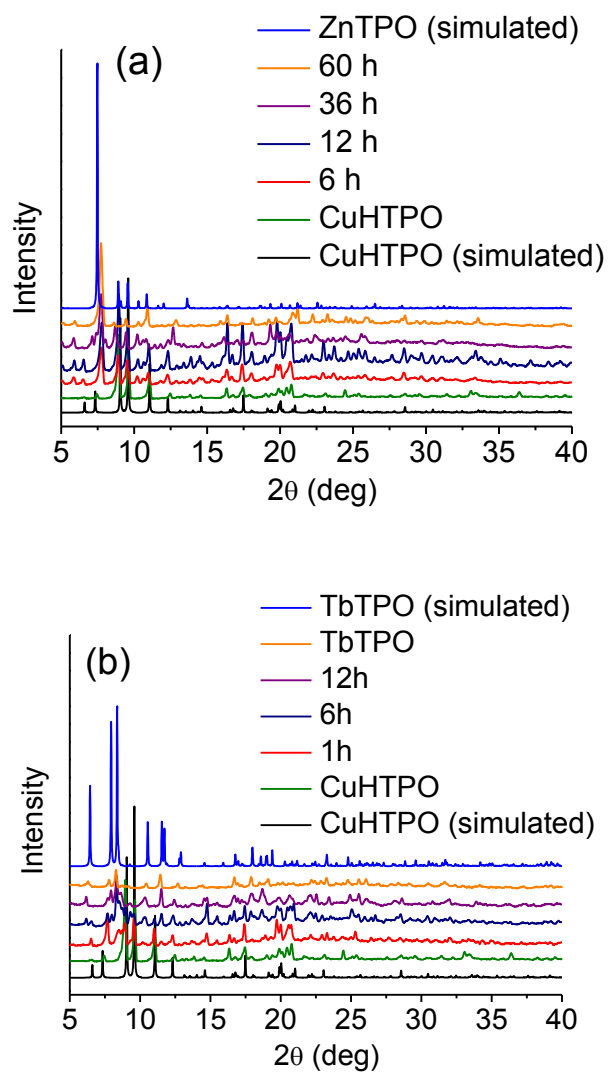
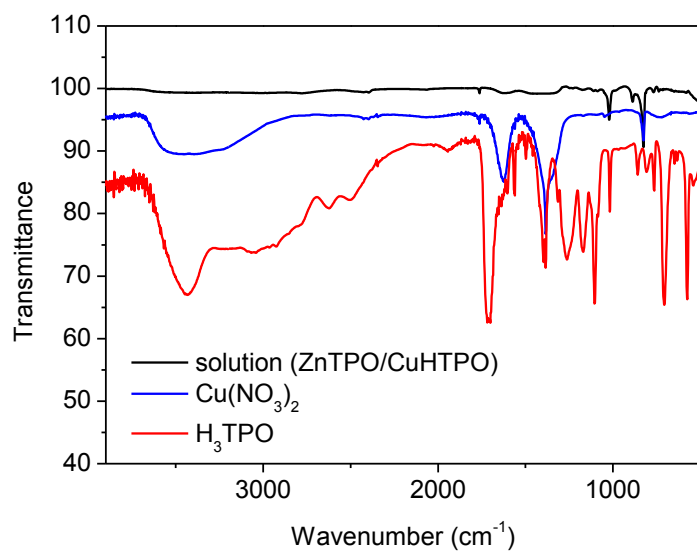Fig. S17. PXRD profiles of (a) **ZnTPO/CuHTPO** and (b) **TbTPO/CuHTPO** crystals.
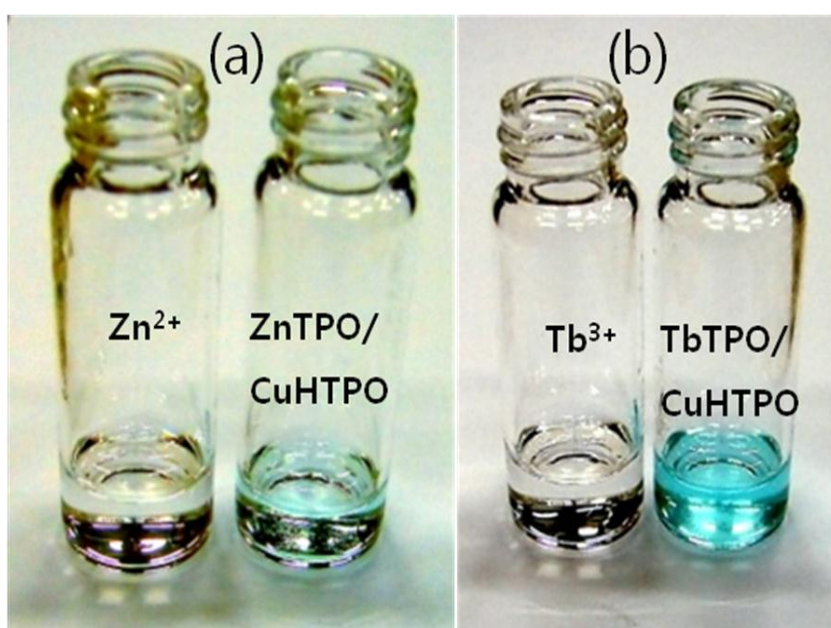
Fig. S18. (a) (left) Solution of 0.5 M $Zn(NO_3)_2$ in DMF:H_2O:MeOH. (right) Filtrate after a solvothermal reaction of **CuHTPO** and Zn^{2+} in DMF/H_2O/MeOH. (b) (left) Solution of 0.5 M $Tb(NO_3)_3$ in DMF/H_2O/MeOH. (right) Filtrate after a solvothermal reaction of **CuHTPO** and Tb^{3+} in DMF/H_2O/MeOH.

(a)
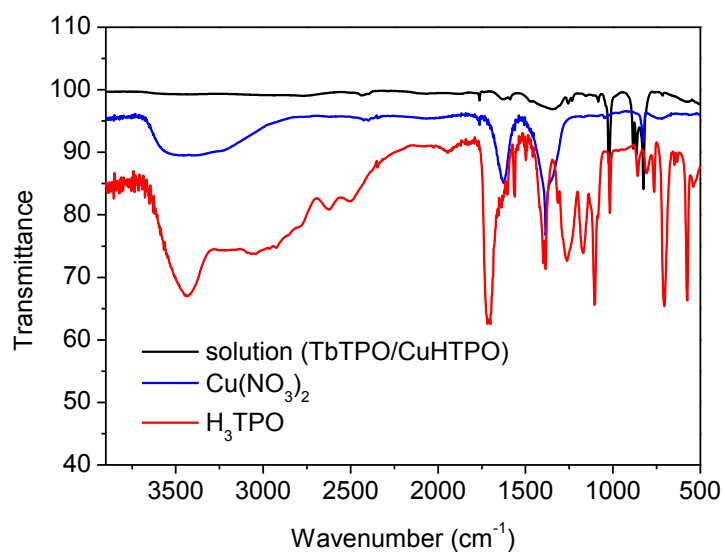
(b)

Fig. S19. IR data of (a) the filtered solution of **ZnTPO/CuHTPO** reaction mixture, $Cu(NO_3)_2$, and H_3TPO, and (b) the filtered solution of **TbTPO/CuHTPO** reaction mixture, $Cu(NO_3)_2$, and H_3TPO.
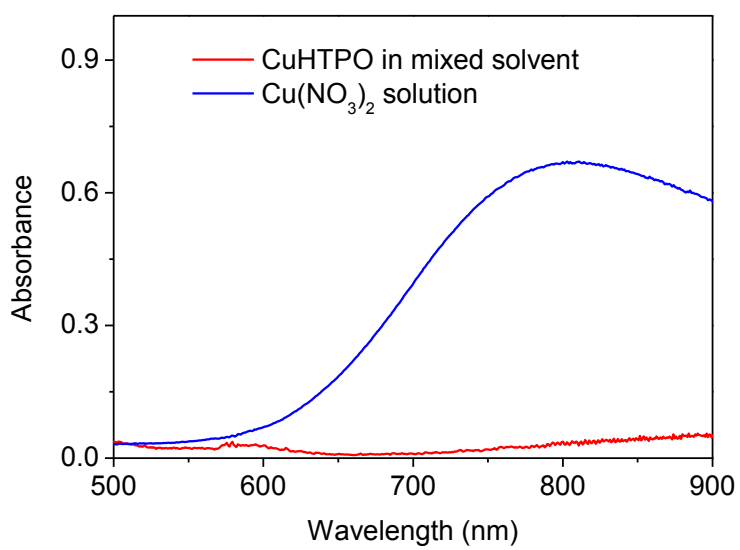
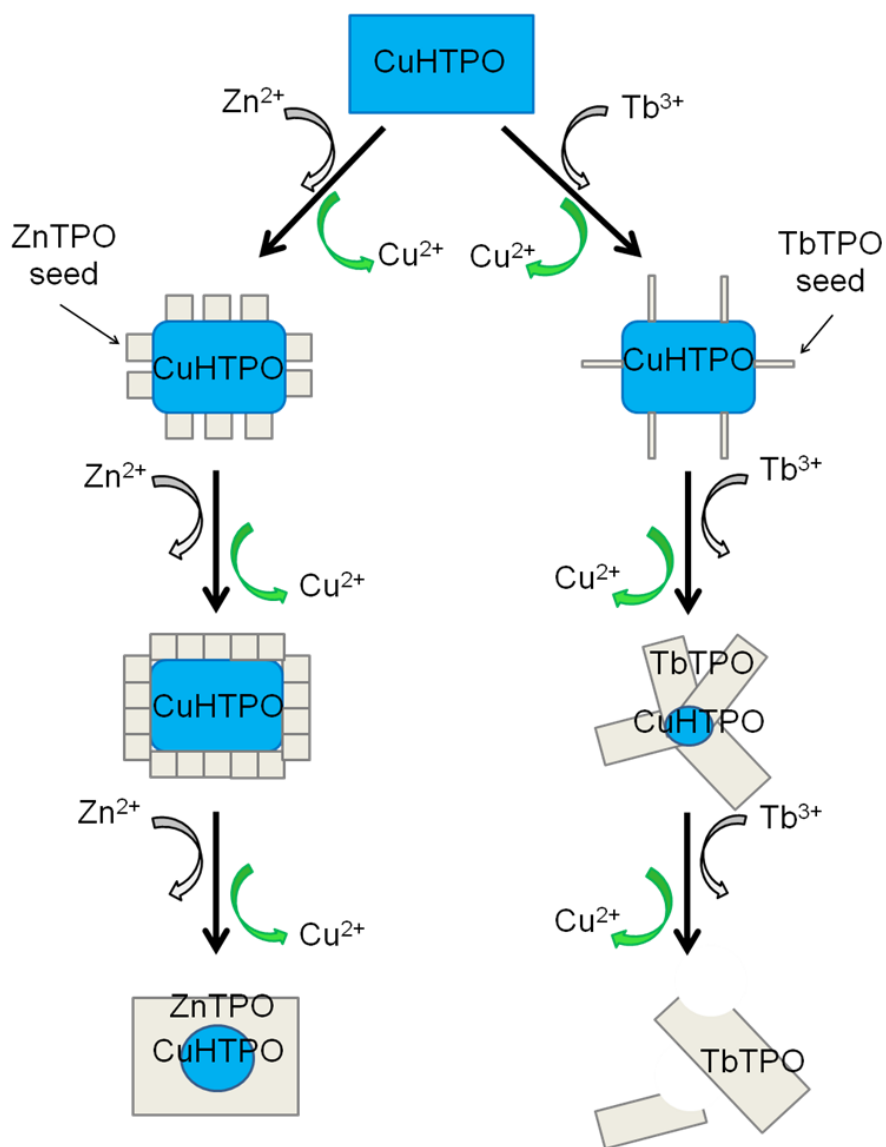Fig. S20. UV/VIS spectra of **CuHTPO** in mixed solvent and Cu^{2+} solution.

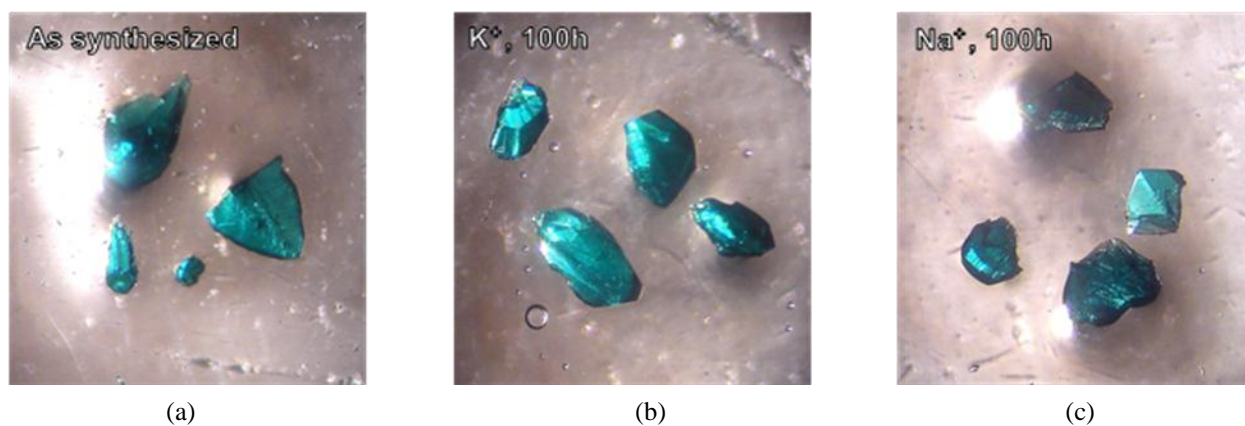Fig. S21. Proposed growth mechanism for the hybridized systems.

| (a) | (b) | (c) |

Fig. S22. Magnified photographs of (a) as-synthesized **CuHTPO** crystals, (b) **CuHTPO** crystals in the K^+ solution, and (c) **CuHTPO** crystals in the Na^+ solution.

Fig. S23. Photographs of CuHTPO crystals in the vials after CuHTPO crystals were treated in the K^+ and Na^+ solution under solvothermal conditions for 100 h.
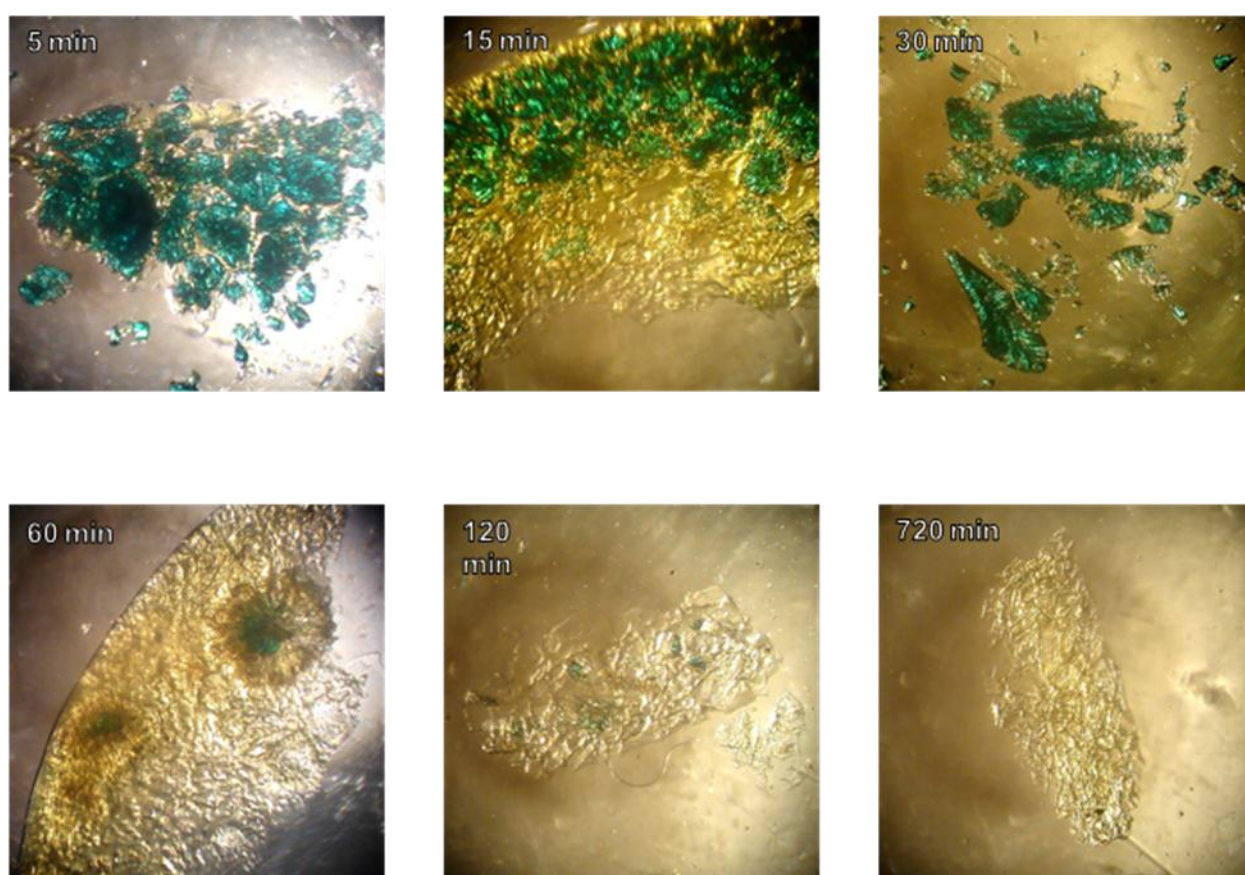
Fig. S24. Magnified photographs of **CuHTPO** crystals immersed in a DMF solution of Zr^{4+} under solvothermal conditions. Most of the **CuHTPO** crystals were collapsed and disappeared at t = 60 min.
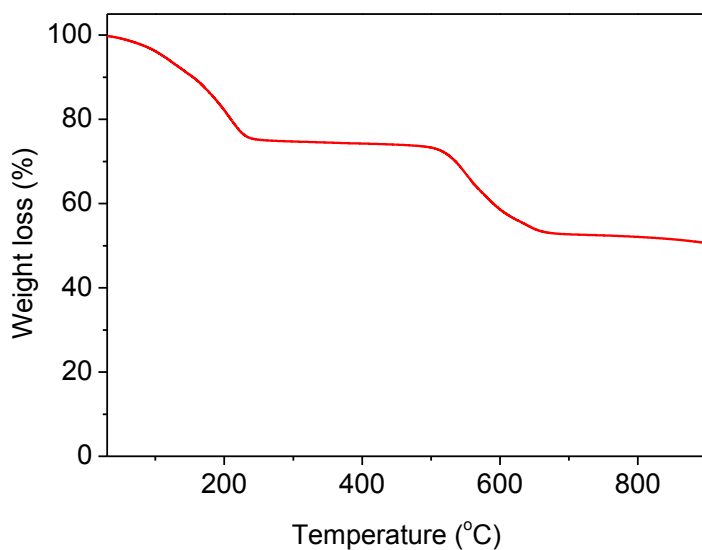
Fig. S25. TGA data for **TbTPO**, showing that the solvent molecules were removed at 240 ^{o}C and the framework was stable up to 520 ^{o}C, above which **TbTPO** started to decompose. Based on the thermal stability, the **TbTPO** sample was activated at 250 ^{o}C under vacuum for 18 h.
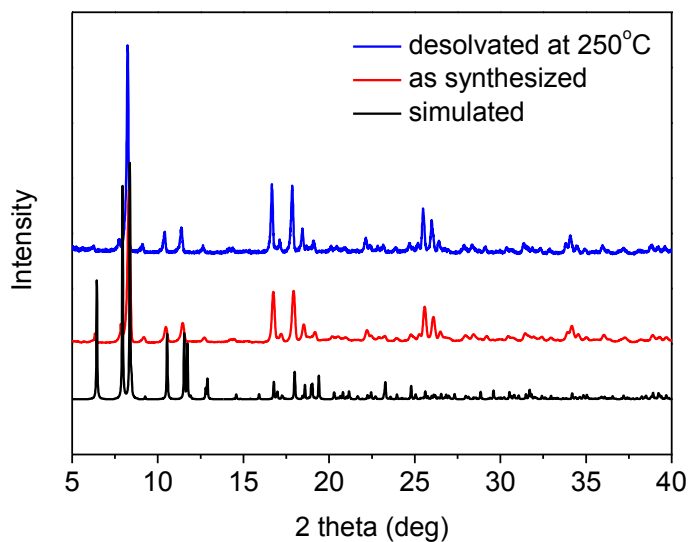

Fig. S26. PXRD profiles for simulated, as-synthesized, and desolvated **TbTPO** at 250 ^{o}C. The structural integrity of the desolvated **TbTPO** was maintained, as checked by PXRD data in which the patterns of the as-prepared and desolvated samples are quite similar.
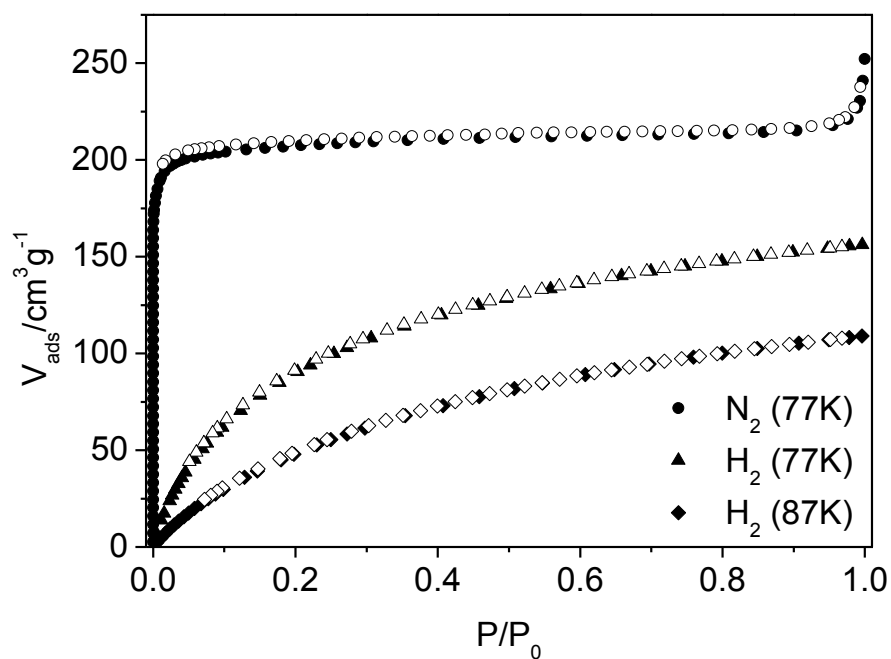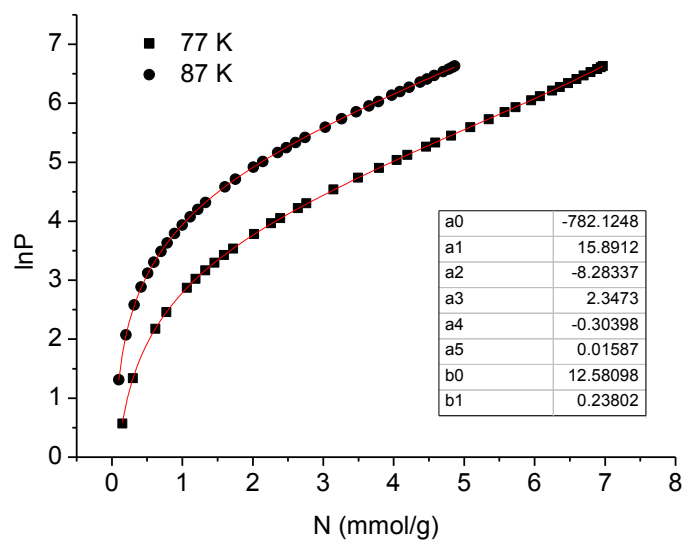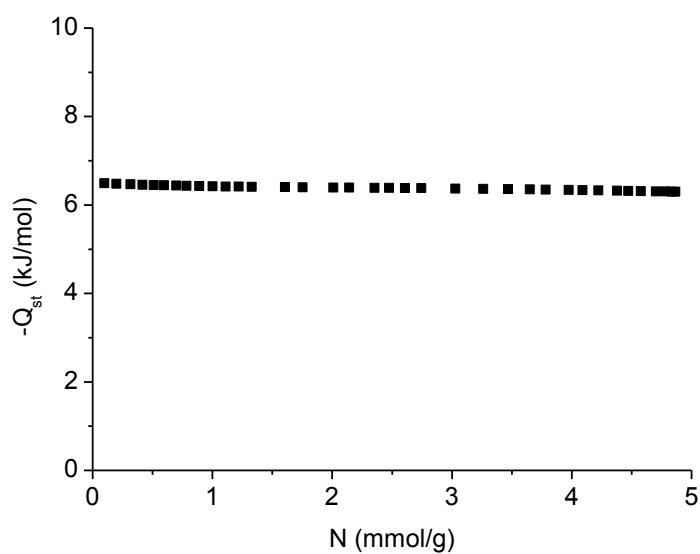
Fig. S27. Adsorption isotherms of desolvated **TbTPO** with several gas molecules. The N_2 isotherm of the evacuated **TbTPO** indicates a normal type I characteristic, which proves permanent porosity of **TbTPO**. The BET surface area and total pore volume are estimated to be 834 m^2/g and 0.35 cm^3/g, respectively. The H_2 uptake at 1 atm and 77 K reaches 6.96 mmol/g (156 cm^3/g) and the number of gas molecules per formula unit is calculated to be 8.3.

a0	-782.1248
a1	15.8912
a2	-8.28337
a3	2.3473
a4	-0.30398
a5	0.01587
b0	12.58098
b1	0.23802

(a)

(b)

Fig. S28. (a) H_2 isotherms at 77 K and 87 K, and virial equation fits for desolvated **TbTPO**. (b) Plot of the isosteric heat of H_2 adsorption for desolvated **TbTPO**. The isosteric heat of adsorption for H_2 is in the range of 6.3 – 6.5 kJ/mol, which is similar to those of TPO-containing lanthanide MOFs.[s8]

s8. W. R. Lee, D. W. Ryu, J. W. Lee, J. H. Yoon, E. K. Koh and C. S. Hong, *Inorg. Chem.* 2010, **49**, 4723-4725.
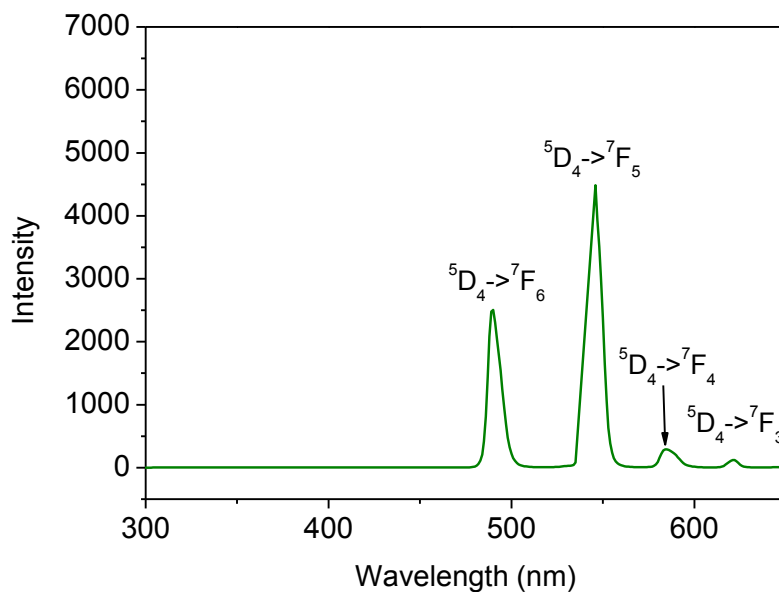
Fig. S29. Emission spectrum for **TbTPO**. The Tb emission peaks were assigned. This gives rise to the strong green luminescence. The characteristic peaks can be assigned to $^5D_4 \rightarrow {}^7F_J$ transitions.
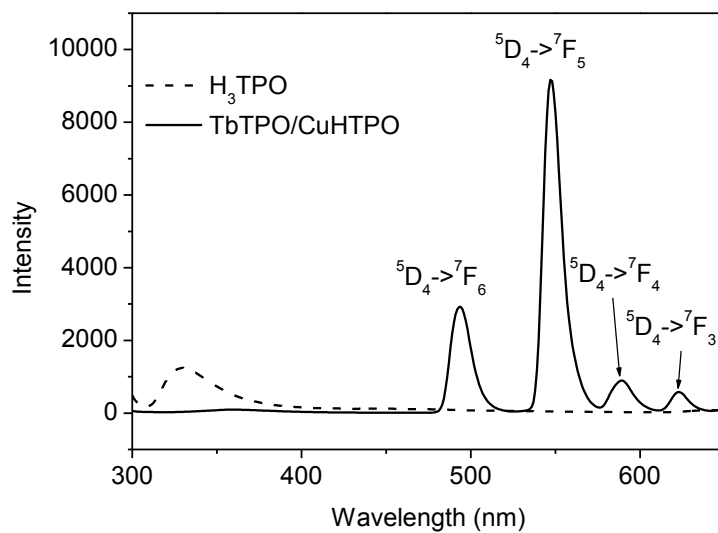

Fig. S30. Emission spectra for H_3TPO (dashed line) and **TbTPO/CuHTPO** at 60 h (solid line). The Tb emission peaks were assigned. The emission profile shows typical Tb^{3+} peaks, which are identical to those of **TbTPO**.
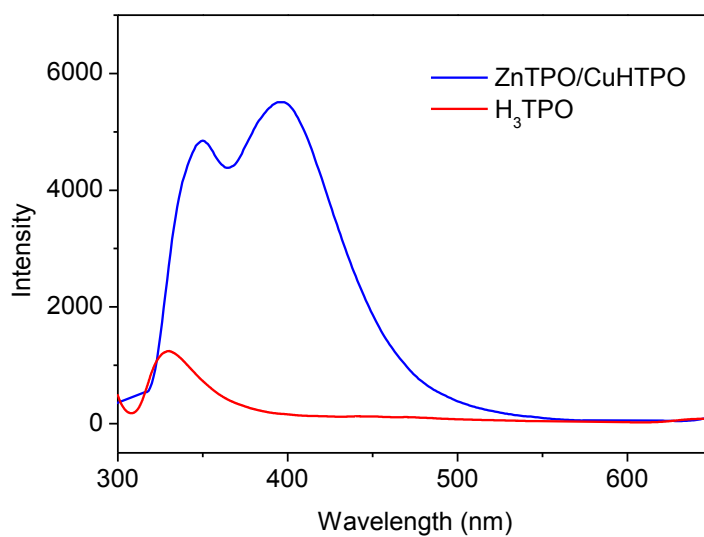
Fig. S31. Emission spectra for H$_3$TPO and **ZnTPO/CuHTPO** at 60 h. In the case of **ZnTPO/CuHTPO**, the luminescence can only arise from **ZnTPO** because paramagnetic Cu^{2+} can quench or reabsorb the emission of **CuHTPO**.